ELSEVIER

Journal of Power Sources 114 (2003) 170–175

JOURNAL OF POWER SOURCES

www.elsevier.com/locate/jpowsour

Short communication

Electron paramagnetic resonance in MnO_2 powders and comparative estimation of electric characteristics of power sources based on them in the MnO_2–Zn system

M. Kakazey[a,b,*], N. Ivanova[c], Y. Boldurev[c], S. Ivanov[d], G. Sokolsky[d], J.G. Gonzalez-Rodriguez[b], M. Vlasova[b]

[a]*Institute for Materials Sciences Problems of Ukrainian National Academy of Science, Krzyzanovsky Str. 3, 252142 Kiev 180, Ukraine*
[b]*Centro de Investigaciones en Ingenieria y Ciencias Aplicadas/FCQI, Universidad Autonomo del Estado de Morelos, Avenue Universidad 1001, C.P. 62210 Cuernavaca, Morelos, Mexico*
[c]*Institute of General and Inorganic Chemistry of Ukrainian National Academy of Science, Palladin Avenue 32-34, 252680 Kiev 142, Ukraine*
[d]*National Aviation University, Cosmonaut Komarov Avenue 1, 04058 Kiev 58, Ukraine*

Received 1 December 2000; received in revised form 29 July 2002; accepted 2 September 2002

Abstract

A study was made of the electron paramagnetic resonance (EPR), the Mn^{3+}/Mn^{4+} ratio, the OH^- groups contents, the ionic conductivity value and the specific capacity in different electrolytically and chemically prepared manganese dioxides which were intended for use in power sources. Typical EPR signal for the powdered MnO_2 samples is wide single line with $g = 1.94$. The replacement of some Mn^{4+} ions by Mn^{3+} modified the character of the exchange interaction. A correlation was established between the width of the EPR signal and electrochemical parameters of the samples. It is supposed that the EPR data can be useful for the semi-quantitative expression of chemical and electrochemical activity of different MnO_2 samples.

Keywords: EPR; MnO_2; Mn^{3+}–Mn^{4+} exchange interactions; Powders; Discharge; Power sources

1. Introduction

Manganese dioxide (MnO_2) is the most extensively used electrode material for different types of power sources (alkaline primary and rechargeable, lithium- and magnesium-based batteries) [1–3]. The dependence of physicochemical properties of MnO_2 on the conditions of its preparation poses the problem of determination of the nature of electronic and defect states defining these properties. This question had been studied thoroughly in [4,5] but a further consideration is required because of the considerable deviation of battery ''active'' manganese dioxide composition from stoichiometry and complexity of its structure. As our previous study [6] shows the structure defects determines electrochemical activity of oxide cathode materials. The measure of the investigated oxides non-stoichiometry was the value of the ionic conductivity. From the obtained results it is possible to conclude that the directed change in defects concentration can be the method of preparation of an active cathode materials, including manganese dioxide.

The electron paramagnetic resonance (EPR) is known as a very important tool of investigation a nature of electronic and defect states in solids [7]. This method is successfully used for the study of different oxide states of manganese [8–12]. In [11], the parameters of an EPR signal in MnO_2—$g = 2.13$, $\Delta B = 176$ mT were presented. Authors in [13] showed that g-factor of the EPR signal of MnO_2 powders (signal A) is equal to 1.94 and their width is depending on quality of samples. The signal A is caused by the Mn^{4+} ions (a $3d^3$ configuration, $S = 3/2$) in MnO_2. The γ-MnO_2 phase is a paramagnetic at room temperature and transforms into an antiferromagnetic state at 92 K. According to the Van Vleck theory [14], the calculated magnitude of the expected width of the line ΔB for the spectrum of Mn^{4+} in MnO_2 is about 430 mT. The smaller magnitude of ΔB for the observed signals is caused by the exchange interaction between Mn^{4+} ions that results in so-called exchange narrowing [7]. The trivalent manganese ions availability into

* Corresponding author.
E-mail addresses: kakazey@hotmail.com, dep8@ipms.kiev.ua (M. Kakazey).

0378-7753/02/$ – see front matter
PII: S0378-7753(02)00595-5

the γ-MnO_2 structure should be explained by the presence of defects [4]. The defects caused by the presence of Mn^{3+} ions in the analogous positions of the MnO_2 lattice stabilized by OH^- groups or other compensators. The partial substitution of tetravalent manganese ions for trivalent ones (a $3d^4$ configuration, $S = 2$) modifies the character of the dipole–dipole interaction and exchange. The kinetic Mn^{4+}–O–Mn^{4+} exchange is typical for the MnO_2 lattice and is antiferromagnetic in character, i.e. $J_{Mn^{4+}-Mn^{4+}} < 0$. The partial substitution of Mn^{4+} ions for Mn^{3+} causes the appearance of one Mn^{3+} ion in the nearest surrounding of Mn^{4+} ions, which have remained at their places. In compounds containing ions of the same element in equivalent positions of their lattices but with different valence, the so-called Zener "double exchange" shows itself [15]. In this case an exchange with an electron takes place between a Mn^{4+} cation and a Mn^{3+} cation separated by an O^{2-} anion: $Mn_1^{3+}-O^{2-}-Mn_2^{4+} \Leftrightarrow Mn_1^{4+}-O^{2-}-Mn_2^{3+}$. This transfer is the result of the two processes: (a) a transfer of a p-electron from the Mn^{3+} cation to the Mn^{4+} cation; (b) a jump of a d-electron from the second cation to its place. Since the spin of the jumping electron in the state with the lowest energy must be equally oriented in relation to S_1 and S_2, this effective indirect exchange is ferromagnetic in a character (in this case $J'_{Mn^{4+}-Mn^{3+}} > 0$). In the general case, the operator of energy of the exchange interaction is written in the form: $E = J_{ef}S_1S_2 = \sum_{j<k}(-2J_{jk}S_jS_k)$. From this expression it can be easily seen that the change of the sign (and the value) of J_{jk} for the part of interacting ions results in the decrease of the absolute value of the effective exchange integral $J_{ef} = J_0 + J'x = J_0(1 + xJ'/J_0)$, where J_0 is the value of the exchange integral in "ideal" MnO_2. The width of the line will change at the small magnitudes of x by the following law:

$$\Delta B(x) \cong \Delta B_0\left(\frac{1 - xJ'}{J_0}\right), \quad (1)$$

where ΔB_0 is the width of the line in the sample free from Mn^{3+}. The comparison of experimental data allowed us to show that $\Delta B_0 \cong 250$ mT and $J'/J_0 \approx -4$ [13].

Was of interest to use the EPR method for the analysis of defect states in a various electrode materials on a base of manganese oxide. In this work a study of the EPR, the concentration Mn^{3+}/Mn^{4+} ratio, the OH^- groups contents, the ionic conductivity value and the specific capacity in different electrolytically and chemically prepared MnO_2 were made. The MnO_2 samples were intended to be used in power sources. It was important to establish a clearer correlation between the EPR signal parameters of the samples and their electrochemical and structural parameters.

2. Samples and experimental procedures

Three samples (1–3) were synthesized by the electrochemical method from a manganese sulfate electrolyte containing different additives of fluoride ions (HF) [16,17]. Another three samples (4–6) were get from commercial sources: sample 4 was obtained by the chemical method, samples 5 and 6 were produced electrochemically (see Table 1). The specific surface areas of the samples were measured by the BET method [18] (Table 1).

Table 1
Origin and specific surface area of MnO_2 samples

Sample no.	Origin	Specific surface area (m^2/g)
1	Electrolytic manganese dioxide produced from fluoride-containing electrolyte [16]: 0.1 M HF	100
2	Electrolytic manganese dioxide produced from fluoride-containing electrolyte [16]: 0.2 M HF	60
3	Electrolytic manganese dioxide produced from fluoride-containing electrolyte [16]: 0.3 M HF	40
4	Chemical manganese dioxide, Pridneprovsk Chemical Plant, Dneprodzerzhinsk, Ukraine	20
5	Serial sample of EMD-2 grade manganese dioxide (OST-6-22-34-76) produced by electrolysis of sulfate electrolyte, Republic of Georgia	20
6	Electrolytic manganese dioxide produced by Kerr–McGee Corp., USA	60

The samples were studied using X-ray diffraction analysis and X-ray phase analysis (DRON-3 diffractometer, Mo Kα-radiation). The data enable us to consider samples 1–6 as a γ-MnO_2, which in the case of samples 1–3 contains insignificant amounts of a α-MnO_2.

The content of Mn^{3+} and Mn^{4+} ions in the samples was determined by chemical analysis. The total manganese in the samples was determined by titration with $KMnO_4$, the Mn^{4+} content being estimated using oxalic acid [19,20]. The difference between the total manganese and Mn^{4+} content (after correction for the actual Mn^{2+} content) corresponds to the experimentally determined value of Mn^{3+} [19–21]. The content of water and OH^- groups in the samples was determined by thermogravimetric analysis using a procedure proposed in [22].

An ionic component of the conductivity was determined by imposing a unipolar rectangular pulse by two-probe method [23]. The discharge tests of manganese dioxide were performed at a constant external loads (0.3, 1.0, and 5.6 kΩ) at room temperature. In this study 450 mg of powder from each sample were mixed thoroughly with graphite (10 wt.%). The resulting active material was pressed under 10 MPa pressure. Taking into account that sample 6 could not be pressed without binder agent we used the minimal possible amount of binder (a Teflon suspension—0.5 wt.%). The thickness of cathode was 1.6 mm. The obtained cathode materials were tested in the coin elements CR1142 (with a diameter of 11 mm and height 4.2 mm) in the system

MnO_2–Zn in an electrolyte containing 9N KOH. The element was assembled in accordance with standard principles [24]. The presence of binder in a sample 6 causes the telemetry error approximately 1 mAh during discharge at the given conditions.

EPR spectra were recorded by 3 cm SE/x-2547 (Radiopan) radiospectrometer equipped with a spectrum analyzer, at both room temperature and 77 K.

3. Results

The EPR spectra recorded in the different MnO_2 samples are shown in Fig. 1. A nearly symmetric single wide line (signal A) with $g = 1.94 \pm 0.02$ is a common feature to all samples. Its width (ΔB) measured between the edge points of the derivative of an absorption signal proved to depend on the type of sample (see Table 2). In some samples six partly resolved symmetrical hyperfine structure (HFS) lines with $g = 2.000 \pm 0.001$, $A = 8.81 \pm 0.05$ mT are superimposed on the line A (signal B in Fig. 1). The employment of the principles of modeling of such spectra, developed previously [25], made it possible to determine the parameters of their spin-Hamiltonian and to estimate ΔB_i of the individual components of the spectrum (Table 2). In work [13] we assigned signal B to $MnSO_4$ aqueous solution in the physically sorbed water localized both on the highly developed surface of MnO_2 particles and in the pores of their aggregates.

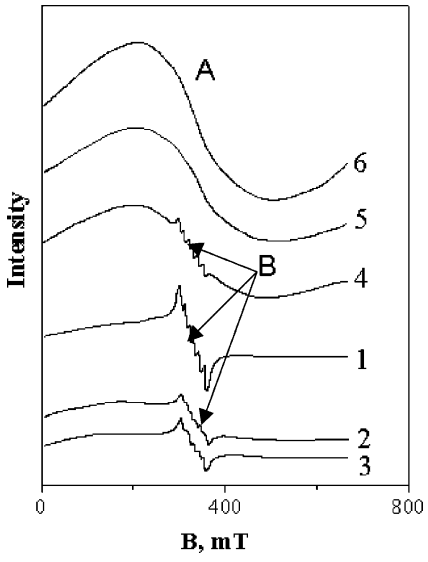

Fig. 1. EPR spectra of MnO_2 samples 1–6 (see Section 3) at room temperature.

Table 2
Experimental parameters of the EPR signals for various MnO_2 samples

Sample	Signal A		Signal B		
	g-factor	ΔB (mT)	g-factor	A (mT)	ΔB_i (mT)
1		375 ± 19			6.8 ± 0.7
2		390 ± 20			7.0 ± 0.7
3	1.92 ± 0.01	418 ± 21	2.000 ± 0.001	8.81 ± 0.05	7.3 ± 0.7
4		292 ± 15			6.0 ± 0.6
5		285 ± 14		Signal B is absent	
6		268 ±14			

The dependence of the line A width (ΔB) on Mn^{3+}/Mn^{4+} concentration ratio in the different samples is plotted in Fig. 2a. This figure reveals a rather clear linear correlation between these data.

Data comparison of line A width with OH^- groups content in the samples is represented in Fig. 2b. The linear dependence of ΔB on OH^- groups content is expected in case of Mn^{3+} ions charges in MnO_2 lattice compensated by OH^- groups (Fig. 2b).

Typical discharge characteristics of MnO_2 cathode of the coin elements CR1142 in 9N KOH electrolyte ($R = 5.6$ and 0.3 kΩ) are shown in Fig. 3. The obtained results demonstrate that time of discharge decreases in the order: $1 > 3 > 2 > 6 > 5 \approx 4$ at a constant external loading 5.6 kΩ. The time of discharge decreases in a similar manner: $1 > 3 > 2 > 6 > 5 \approx 4$ at $R = 1$ kΩ. This order is changed at loading 0.3 kΩ: $3 > 1 \approx 2 > 5 \approx 4 > 6$. It is shown that the discharge voltage is maximal for sample 6 produced in Kerr–McGee Corp. at the investigated range of loadings.

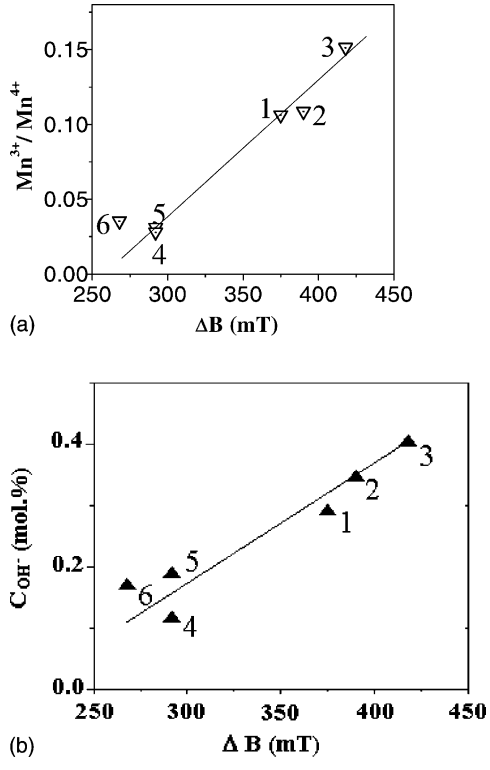

Fig. 2. Correlation of EPR signal A width (ΔB) with the Mn^{3+}/Mn^{4+} ratio (a) and content of OH^- groups (b) in the investigated samples 1–6.

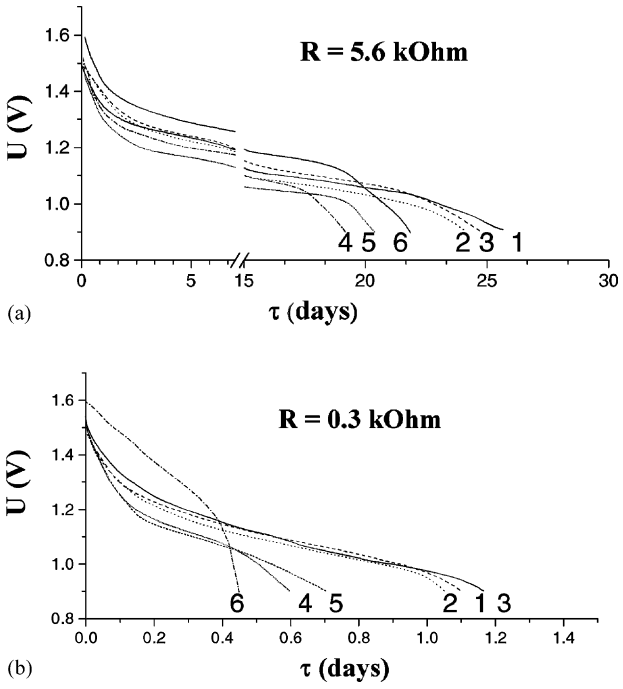

Fig. 3. Discharge curves of MnO_2 cathodes (samples 1–6) of the coin elements CR1142 in 9N KOH electrolyte: (a) $R = 5.6$ kΩ; (b) $R = 0.3$ kΩ.

The comparison of the ionic conductivity σ_{ion} data with the line A width in the samples is shown in Fig. 4a. The latter confirms the linear correlation between them.

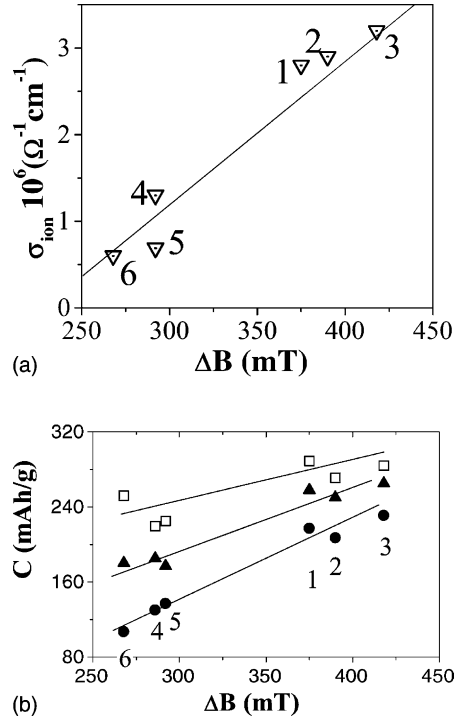

Fig. 4. Correlation of EPR signal A width (ΔB) with ionic conductivity (a) and specific capacity of MnO_2–Zn alkaline coin elements (b) in the investigated samples 1–6. For (b): $R = 5.6$ kΩ (□); $R = 1$ kΩ (▲); $R = 0.3$ kΩ (●).

The specific capacity data measured in the samples at different loading in comparison with the line A width in them are shown in Fig. 4b. It also represents the important correlation between these data.

4. Discussion

From the point of view of a pure magnetic interaction, the nature of non-magnetic centers–compensators in samples MnO_2 weakly influences the signal A width in them. As it was shown in [13], ΔB is determined by the Mn^{3+}/Mn^{4+} ratio. The comparison of the EPR data with data of other measurements shows that there is a rather clear correlation between the width of line A and the Mn^{3+}/Mn^{4+} ratio (Fig. 2a). The observable linear correlation $\Delta B(Mn^{3+}/Mn^{4+})$ is described by expression (1). The smaller signal A width in sample 6 compared with samples 4 and 5, at the little bit greater value of Mn^{3+}/Mn^{4+} ratio, apparently, could be explained by the distinction in the samples surface area (60 m^2/g for sample 6 and 20 m^2/g for samples 4 and 5). The last mentioned differentiation exerts influence both on the precision of the measurements and on peculiarities of Mn^{3+} centers distribution in particle volume. For instance, the main contribution to the registered EPR signal A width at preferable surface localization of Mn^{3+} centers give Mn^{4+} ions distributed in particles bulk where the concentration of Mn^{3+} centers is lower. It means that the registered signal width in such sample should be lower, than in a sample with uniform distribution of Mn^{3+} centers.

Apparently, by distinction in a surfaces can explain the fact that sample 6 has the higher value of capacity at $R = 5.6$ kΩ than samples 4 and 5 what expected according to the signal A widths (Fig. 4b). The same conclusion can be made for sample 1 and similar samples 2 and 3. However, the capacity values of these samples at low loading (0.3 kΩ) are in better agreement with the EPR data (Fig. 4b).

The discharge curves analysis at different loading deserves a special attention (Fig. 3). At homogeneous distribution of electroactive centers in particle volume of the samples, it is possible to expect rather typical behavior of these curves at different loading for samples with various concentrations of active centers. The observed deviation of the discharge curves order at different loading (especially in case of sample 6; Fig. 3), apparently, should be explained by the distinction in surface area of the samples mentioned above and also by inhomogeneity of electroactive centers Mn^{3+} distribution in particles volume. At preferential localization of Mn^{3+} centers at the surface such sample at high loading (in this case the main channels of mass transfer are the surface states) behaves as a sample containing considerably higher concentration of centers at their uniform distribution in the particles volume. At low loading all electroactive centers participate in the mass transfer and the discharge curves behavior follows the defects concentration in samples.

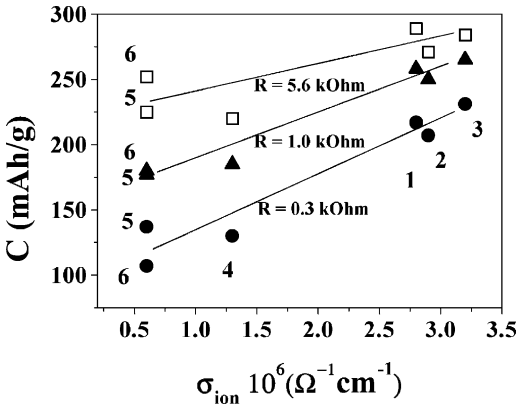

Fig. 5. Correlation of specific capacity of MnO_2–Zn alkaline coin elements with ionic conductivity in the investigated samples 1–6: $R = 5.6$ kΩ (□); $R = 1$ kΩ (▲); $R = 0.3$ kΩ (●).

Based on our consideration, it is evident that different mechanisms of mass transfer could be realized at different loading. At high loading, the complete electroreduction of the surface states proceeds at first and then the mass transfer process gradually moves into the bulk of a cathode material. At low loading, when the values of current are large, the defect states of the particles volume immediately participate in electroreduction and define the rate and activity of samples (see also below). This does not necessarily mean that such dependence does not exist at other loading, but the best agreement of our results can be seen at the low ones.

It should be emphasized that samples obtained from fluorine containing electrolytes can be discharged at low external loadings (about 1 kΩ) with high values of capacity (Figs. 4b and 5). It can be observed from Fig. 2 that these samples have the largest concentration of defect positions. The other advantages of these electrode materials for power sources are simple production [16] and the absence of Teflon binder in cathode material.

Comparing the results of both the physicochemical measurements and discharge tests of the investigated manganese dioxide samples, it might be concluded that the number of lattice defects—Mn^{3+} and OH^- compensator concentrations—increased the sample capacity. We suppose that structure defects considered could be the cause of the faster H^+ ions transport during discharge by means of the exchange mechanism. The contribution of such mechanism in the reduction process can be estimated by the ionic conductivity value as a result of charge carriers self-diffusion in a sample [26]. It is known that the absolute value of the ionic conductivity depends on the concentration of charge carriers and their mobility by the following law [26]:

$$\sigma_{\text{ion}} = qxN\mu, \tag{2}$$

where q is the charge, x the mole fraction of defects, N the number of ions per unit of volume and μ the mobility. In oxides of non-stoichiometric composition OH^- group is the main carrier of ionic charge. The latter can be confirmed by the specific capacity (ionic conductivity) dependence (Fig. 5).

Actually, a rather clear correlation between electrochemical and EPR data is observed (see Figs. 4b and 5). Thus, dependencies presented can be practically used as an estimation of the expected specific capacity values according to ΔB data of different MnO_2 samples. It is proposed to use EPR data for the testing and semi-quantitative expression of chemical and electrochemical activity of different MnO_2 compounds. Electrical parameters of testing elements have confirmed this conclusion.

5. Conclusion

In the EPR study of the electrolytically and chemically prepared MnO_2 powder samples we established that a broad singular line A with $g = 1.94$ is typical. A hyperfine signal B also appeared in some samples ($g = 2.000$, $A = 8.81$ mT). The latter is caused by Mn^{2+} ions of $MnSO_4$ aqueous solution in the water physically adsorbed that are localized both on the highly developed surface of MnO_2 particles and in the pores of their aggregates. The analysis shows that the width of signal A is due to the presence of the dipole–dipole and exchange interaction between Mn^{4+} ions. The partial substitution of Mn^{4+} ions for Mn^{3+} modifies the character of the interaction and causes the broadening of the recorded signal. The good correlation between the width of signal A in different samples and the Mn^{3+}/Mn^{4+} ratio was established. The linear dependence of ΔB_A and the content of OH^- groups, the value of the ionic component of conductivity as well as the samples capacity are also observed in case of Mn^{3+} ions into MnO_2 lattice compensation by OH^- groups. The observable dispersion of the data for samples with close concentration Mn^{3+} ions (samples 1–6) are connected to distinction in a surface of samples and also with heterogeneous distribution of ions in particles.

Our results show that EPR data can be the measure of defects concentration, which are responsible for electrochemical activity of manganese dioxide samples. It is proposed to use EPR data for the testing and semi-quantitative expression of chemical and electrochemical activity of manganese dioxide in power sources.

The important advantages of samples 1–3 are the ability of discharge at low external loads (about 1 kΩ) simple production and the absence of binder in cathode material.

References

[1] B.D. Desai, J.B. Fernandes, V.N. Kamat Dalal, J. Power Sources 16 (1985) 1.
[2] K. Takahashi, Electrochim. Acta 26 (1981) 1467.
[3] G. Piao, M. Yoshio, H. Noguchi, A. Kozawa, J. Power Sources 51 (1994) 391.
[4] J. Brenet, J. Power Sources 4 (1979) 183.
[5] P. Ruetschi, R. Giovanioli, J. Electrochem. Soc. 135 (1988) 2663.
[6] N. Ivanova, E. Boldyrev, G. Sokolsky, in: Proceedings of the 50th ISE Meeting, Pavia, Italy, 5–10 September 1999, p. 681 (Abstract).

[7] A. Abragam, B. Bleany, Electron Paramagnetic Resonance of Transition Ions, Oxford University Press, Oxford, 1970.
[8] L.R. Mawell, T.R. McGuire, Rev. Mod. Phys. 25 (1953) 279.
[9] J.W. Battles, J. Appl. Phys. 42 (1971) 1286.
[10] E. Dormann, V. Jaccarino, Phys. Lett. 48A (1974) 81.
[11] M.S. Seehra, G. Srinivasan, J. Appl. Phys. 53 (1982) 8345.
[12] J. Uebersfeld, C. R. Acad. Sci. 237 (1953) 1645.
[13] M. Kakazey, N. Ivanova, G. Sokolsky, G. Gonzalez-Rodriguez, Electrochem. Solid State Lett. 4 (2001) N5J1–N5J4.
[14] J.H. Van Vleck, Phys. Rev. 73 (1948) 1249.
[15] C. Zener, Phys. Rev. 118 (1951) 403.
[16] N.D. Ivanova, E.I. Boldurev, I.S. Makeeva, G.V. Sokollsky, Jurn. Prykl. Chem. 71 (1998) 121 (in Russian).
[17] S.A. Zaretzky, V.N. Suchkov, V.A. Shlyapnikov, Technology of Electrochemical Manufacturing, Vusshaya Shkola, Moscow, 1970 (in Russian).
[18] S. Brunauer, P.H. Emmett, E.J. Teller, J. Am. Chem. Soc. 60 (1938) 309.
[19] A.I. Vogel, Quantitative Inorganic Chemical Analysis, Longmans & Green, London, 1961.
[20] K.M. Parida, S.B. Kanungo, B.R. Sant, Electrochim. Acta 26 (1981) 435.
[21] D. Glover, B. Schumm, A. Kozawa, Handbook of Manganese Dioxide Battery Grade, International Union of Battery Materials Associations, Inc., 1989.
[22] K.M. Parida, S.B. Kanungo, Thermochim. Acta 66 (1983) 275.
[23] B. Zelutska, Z. Ogorelec, J. Phys. Chem. Solids 27 (1966) 957.
[24] R.J. Brodd (Ed.), Batteries for Cordless Appliances, Research Studies Press Ltd., Letchworth, Hertfordshire, UK, 1987.
[25] Y.S. Lebedev, V.V. Voevodsky (Eds.), Atlas Electron Paramagnetic Resonance Spectra, AS USSR, Moscow, 1962 (in Russian).
[26] W.E. Garner (Ed.), Chemistry of the Solid State, Butterworths, London, 1955.